Pharmaceutical Sciences Asia

Pharm Sci Asia 2025; 52(4), 471-482

DOI:10.29090/psa.2025.04.25.3941

Research Article

# Development and characterization of ceftazidime-loaded niosomes against selected pathogens

Jan Karlo Tiongson Ecalne[1,3*], Gerard Quinto De Guzman[2], Saffia Anzures Abu-Shendi[1], Justin Dave Magracia Manantan[3*], Jan Ken Emmanuel Tiongson Ecalne[1], Mylene Sevilla Andal[1]

[1] School of Pharmacy, Centro Escolar University – Manila, 9 Mendiola Street, San Miguel, Manila, 1008, Philippines
[2] College of Medicine, University of the Philippines – Manila, 670 Padre Faura Street, Ermita, Manila, 1000, Philippines
[3] College of Pharmacy, Adamson University, 900 San Marcelino Street, Ermita, Manila, 1000, Philippines

## ABSTRACT

Ceftazidime (CP) is a third-generation bactericidal cephalosporin used to treat infections, such as pneumonia and meningitis. Despite its clinical use, the emerging threat of antimicrobial resistance makes the drug questionable. This study aims to entrap CP into niosomes, providing a unique mechanism for enhancing its antibacterial activity against selected pathogens. Five niosomal formulations with varying molar ratios of surfactant were prepared and tested for *in vitro* release and entrapment efficiency (EE). The most favorable formulation was further characterized using scanning electron microscopy (SEM), particle size (PS), polydispersity index (PDI), zeta potential (ZP), Fourier transform infrared spectroscopy (FTIR), and differential scanning calorimetry (DSC). A three-month accelerated stability study was also conducted to determine its suitability under common storage conditions. The antibacterial activity against selected pathogens was assessed using the agar well diffusion method. The formulation containing the highest molar ratio of Span 60 was selected due to its superior entrapment efficiency ($72.49 \pm 0.23\%$) and diffusion performance ($804.8 \pm 145.4$ µg/hr). This optimized formulation exhibited a spherical, vesicular morphology with favorable particle size, polydispersity index, and zeta potential. FTIR and DSC analyses confirmed successful entrapment of the active compound, while minimal changes in entrapment efficiency, zeta potential, and pH under cold storage indicated relative stability. Moreover, it demonstrated enhanced antibacterial activity against *Klebsiella pneumoniae*, *Pseudomonas aeruginosa*, and *Staphylococcus aureus* compared to the free drug. This study was the first to report that niosomal entrapment improves CP's antibacterial activity, establishing a framework for future advances in antimicrobial drug delivery.

**Keywords:**
Niosome; Ceftazidime; Nosocomial; Bactericidal; Antimicrobial resistance

## 1. INTRODUCTION

Antimicrobial resistance (AMR) to commercially available agents has been a rising global health concern. Public health organizations warn that the rapid spread of AMR internationally may result in a "post-antibiotic era" in the twenty-first century[1]. AMR undermines effective antibiotic management by spreading resistant microorganisms throughout communities, raising treatment costs. Recent studies have highlighted various factors contributing to AMR, including natural selection, antibiotic abuse and misuse, poor sanitation and hygiene, and the spread of substandard or counterfeit drugs[2]. This necessitates the search for newer options, such as drug combinations, and developing novel systems using commercially available drugs to produce safer and more effective drug delivery to reduce the risk of resistance[3,4].

***Corresponding author:**
* Jan Karlo Tiongson Ecalne Email: jtecalne@ceu.edu.ph

Nanocarriers such as niosomes have shown great potential in enhancing the delivery of antimicrobial agents, thereby contributing to the reduction of antimicrobial resistance (AMR), as highlighted by Barani et al.[4]. Niosomes offer several advantageous features: a micronized size that facilitates penetration through cell membranes, a lipid bilayer structure that enables efficient drug encapsulation, a hydrophobic character that promotes interaction with bacterial membranes, and a vesicular structure capable of encapsulating both hydrophilic and lipophilic drugs —allowing for the delivery of a wide range of antimicrobial agents[4,5]. Barani et al. also reported that charged niosomes can interact electrostatically with bacterial cell walls, further enhancing their targeting ability. Furthermore, niosomes can be functionalized with specific ligands such as chitosan, lactoferrin, or plant-derived compounds like curcumin, depending on the target pathogen and therapeutic goals. Supporting these findings, Paseban et al. developed meropenem-loaded niosomes that exhibited four- to six-fold greater activity against methicillin-resistant *Staphylococcus aureus* (MRSA) compared to the free drug[6]. Similarly, Shiri et al. encapsulated berberine into niosomes, which demonstrated a minimum inhibitory concentration (MIC) of 80 μg/mL against *Staphylococcus aureus* and *Escherichia coli*[7].

Ceftazidime (CP) is a third-generation cephalosporin widely used to treat nosocomial infections such as meningitis, pneumonia, and other tissue infections. Its parenteral preparations are included in the latest editions of the British and the United States Pharmacopoeias, and they are classified as essential medicine in the Philippine National Drug Formulary (PNDF). Despite its low protein-binding capacity and high bioavailability, CP has a short half-life of less than two hours. The drug is becoming increasingly resistant in many settings, including neonatal and pediatric infections, intensive care units, and burn centers.

Niosomes have been shown to form a concentration gradient within the cell membrane of pathogenic bacteria, resulting in sustained drug release and biofilm eradication[5]. They can also protect the drug against beta-lactamase and inhibit p-glycoprotein, which promotes further absorption[8]. These factors make them an ideal carrier for CP and other antibacterial agents. This study aims to provide an innovative drug delivery for CP by characterizing its niosomal formulation and evaluating its antibacterial activity against selected nosocomial pathogens.

## 2. MATERIALS AND METHODS

### 2.1. Materials

CP (95%-102% purity) as the substrate and dicetyl phosphate (≥ 95% purity) were purchased from Chem-Impex International, Inc. (Illinois, USA). CP (USP RS) as the standard was purchased from AE Alchemists, Inc. (Bulacan, Philippines). Span 60, cholesterol, and dicetyl phosphate (DCP) were purchased from Sigma-Aldrich (Missouri, USA).

### 2.2. Drug-excipient compatibility

An equimolar (1:1) ratio of CP with each of the excipients was mixed and then placed in screw-capped amber bottles before being stored at cold (2°C – 8°C) and controlled room (20°C – 25°C) temperatures for one month. The IR spectra were then acquired using a Fourier Transform Infrared (FTIR) spectrophotometer (IRSpirit-T™, Shimadzu, Taguig, Philippines). The IR spectrum was recorded by placing a small amount of each sample on the ATR crystal surface. The spectrum was measured by collecting 20 scans with a resolution of 4 $cm^{-1}$ across a wavenumber range of 4000 $cm^{-1}$ to 500 $cm^{-1}$. The spectrum was analyzed with LabSolutions™ IR software, and the results were given as percentage (%) transmittance. The absence of significant variations in the vibrations of the samples over the entire period will determine the relative compatibility between the drug and excipients.

### 2.3. Preparation of niosomes

The niosomes were prepared using the thin film method outlined by Bagheri et al. with some modifications[9]. 10 mL of chloroform was added to a 500-mL round-bottom flask containing carefully weighed span 60, cholesterol, and DCP. A rotary evaporator (RV 10®, IKA, Selangor, Malaysia) was used to remove the organic solvent at 60°C and 200 rotations per minute (rpm) for 30 minutes until a thin film formed in the inner wall of the flask. A mixture of 100 mg CP in 10 mL of phosphate-buffered saline (PBS) with a pH of 7.4 was added to the flask. The mixture was placed in the rotary evaporator at normal pressure for 50 minutes to facilitate complete hydration. The initial dispersion was stored overnight at 4°C, then subjected to a bath sonicator at 60°C for 2 minutes, forming multilamellar niosomes. **Appendix A** presents the composition of the blank niosomes and five formulations containing varying molar ratios of Span 60 that were prepared and evaluated. Cholesterol and DCP are maintained at an equimolar ratio because excessive cholesterol levels can disrupt vesicle uniformity, strength, and permeability by promoting cluster formation[10], while high DCP concentrations can inhibit niosomal formation due to electrical charges generated by membrane curvature modifications[11].

### 2.4. Entrapment efficiency (EE)

The unentrapped CP was separated from the prepared niosomes by ultracentrifugation. 1 mL of the

niosomal dispersion was placed in Eppendorf tubes and centrifuged (Sorvall™ ST 8, Thermo Fischer Scientific, Massachusetts, USA) for 1 hour at 15,000 rpm and 4°C. The supernatant liquid was removed before washing the niosomes twice with 1 mL of PBS and centrifuged under the same conditions. To release the CP from the niosomal vesicles, 100 µL of the mixture was deposited in a small test tube using a micropipette and then lysed with 1 mL of n-propanol separately. PBS was added to make a 10 mL volume. A UV-Vis spectrophotometer (UV-1280, Shimadzu, Taguig, Philippines) was used to measure the absorbance of the prepared mixture at 210 nm, with the amount of entrapped drug calculated using linear regression analysis of the previously performed calibration curve.

The equation below was used to calculate the entrapment efficiency (EE), where $C_2$ and $C_1$ represent the amounts of drug entrapped in the niosomes and drug utilized to prepare the niosomes, respectively. The values were then expressed as a percentage (%).

$$EE = \left(\frac{C_2}{C_1}\right) x\ 100$$

The ability of surfactants to self-assemble is essential for producing well-formed vesicles. This property is represented by the minimization of Gibb's free energy, which indicates the spontaneous solubilization of CP in niosomal vesicles[12]. The parameter (ΔG°) was computed using the equation below, where R denotes the universal gas constant and T represents the absolute temperature in Kelvin[13]. The results were provided as kilocalories per mole (kcal/mol).

$$\Delta G° = -2.303 * R * T * \log\left(\frac{C_2}{C_1}\right)$$

## 2.5. *In Vitro* Drug Release Studies

The release of CP from niosomes was evaluated using the work of Zaki et al., which employed a USP Dissolution Apparatus 1 (DT 950, Erweka, Langen, Germany)[14]. A cellulose membrane was soaked for 10 minutes in distilled water at 40°C before being cut to cover the basket assembly that will serve as the donor compartment. Glass tubes were securely connected to the open ends of each basket assembly to prevent leakage. Each basket assembly received a particular volume of formulations 1–5, equivalent to 50 mg of CP. To ensure complete submersion, the basket assemblies were attached to their respective rotating shafts and positioned 4 cm below the bottom surface of their dissolution vessel. Each dissolution vessel contained 500 mL of PBS to act as the receptor compartment. The basket assembly was rotated at 100 rpm, with the dissolution medium kept at 37 ± 0.5°C. 1 mL of aliquot was taken from each vessel every hour for 8 hours and immediately replaced with fresh medium. The absorbance of each sample was measured at the same wavelength using a UV-Vis spectrophotometer. The amount of CP released from the donor compartment was calculated using the same formula as the calibration curve.

The amount of CP released was then plotted against time and fitted to various kinetic models to determine the possible release mechanism, as outlined in **Appendix B**. In these models, C = drug concentration at time *t*, $C_0$ = initial drug concentration, k = rate constant, Q = cumulative amount of drug released at time *t*, $k_H$ = Higuchi rate constant, $t^{½}$ = square root of time, $M_t$ = amount of drug released at time *t*, $M_\infty$ = total amount of drug released at infinite time, $k_K$ = Korsmeyer-Peppas rate constant, and n = diffusional coefficient.

The diffusion efficiency (DE) of each niosomal formulation was compared using the published formulas for difference ($f_1$) and similarity ($f_2$) factors by Zaki et al.[14]. The formulation with the most favorable results for drug encapsulation and diffusion efficiency will be referred to as the optimized niosomal formulation (ONF) of CP and will be further investigated.

## 2.6. Solid state analysis

The ONF underwent the following tests to characterize its behavior and properties as solids:

### *2.6.1. Scanning electron microscope (SEM)*

The ONF was placed in a double-sided carbon tape previously affixed to the sample stub and was coated with gold at a reduced pressure of 0.001 mmHg until it reached a thickness of 200 nm. The surface morphology was observed at different magnifications using a 10 kV accelerating voltage (JSM-5310™, JEOL Ltd., Tokyo, Japan).

### *2.6.2. Particle size (PS) and polydispersity index (PDI) analysis*

The ONF was diluted hundredfold with distilled water before being placed in a glass cuvette to be measured for PS and PDI using a nanoparticle analyzer (NanoPlus HD™, Micromeritics®, Georgia, USA) at 25°C and 90° angle.

### *2.6.3. Zeta potential (ZP)*

The ZP was measured in triplicate using a zeta potential analyzer (Zeta-Meter 4.0, Zeta-Meter, Inc., Virginia, USA) based on electrophoretic mobility. The ONF (2% w/v) was placed in an electrophoresis cell and analyzed with a 30 V applied voltage.

*2.6.4. FTIR analysis*

An FTIR spectrophotometer (IRSpirit-T™, Shimadzu, Taguig, Philippines) was used to identify the vibrations of the functional groups present in the various components of the niosomes, with successful entrapment of CP demonstrated by detecting only the vibrations of the functional groups present in the niosomal structure.

**2.7. Differential scanning calorimetry (DSC) analysis**

5 mg of each sample (CP, ONF, blank niosomes) was weighed using an analytical balance before placing it in an aluminum pan for testing (DSC 6000, PerkinElmer®, Massachussets, USA). The sample was heated at 5°C per minute from 10°C to 400°C while receiving a nitrogen flow of 25 mL per minute. The data was analyzed using a software provided with the instrument (Pyris™, PerkinElmer®, Massachussets, USA).

**2.8. Stability testing**

Six batches of ONF were placed in tight, glass tubes. Three were stored at cold temperatures, while the others were kept in a stability oven at a controlled room temperature and 75 ± 5% RH for three months. The samples were tested for EE, ZP, pH, SEM, and FTIR analyses at the end of each month.

**2.9. Antibacterial assay**

The experiment was conducted at the University of the Philippines (Diliman, Quezon City, Philippines). The assay included four pathogenic strains of *Escherichia coli* (ATCC BAA-2452), *Staphylococcus aureus* (ATCC BAA-1708), *Pseudomonas aeruginosa* (ATCC 27853), and *Klebsiella pneumoniae* (ATCC BAA-1705). The test pathogens were initially cultivated in Mueller-Hinton Agar (MHA) and then transferred to 0.1% peptone water with turbidity set to 0.5 MacFarland units.

The bacterial agar was prepared using the streak plate method, which involves streaking each test inoculum to the entire surface of pre-poured MHA plates with a cotton swab into an applicator stick. The procedure was repeated twice, with the plate rotated to 60° to ensure even distribution of the inoculum. A sterilized cork borer was used to drill three equidistant 10 mm diameter wells in each plate. The blank niosomes, 0.05% w/v CP, and ONF with the same drug concentration were diluted with PBS. 200 µL of each sample into the separate wells using a microtiter pipet. The plates were incubated (DRP-9082, Nade®, Zhejiang, China) for 24 hours at 37°C before being inspected for zones of inhibition (ZOI). The ZOI was measured with a digital Vernier caliper and reported in millimeters (mm).

**2.10. Statistical analysis**

The tests were performed in triplicates, and the results were expressed as the mean ± standard error (SE) of the mean. A t-test was employed to determine significant differences in activity between samples and positive controls ($p < 0.05$).

**3. RESULTS AND DISCUSSION**

**3.1. Drug-excipient compatibility**

The FTIR spectrum in **Appendix C** detects the presence of each component in the formulation. The C-H vibrations at 2955.8 $cm^{-1}$, 2929.7 $cm^{-1}$, 2918.5 $cm^{-1}$, and 2914.8 $cm^{-1}$ suggest the presence of aliphatic groups in all excipients. O-H vibration at 3101.2 $cm^{-1}$ suggests the presence of an alcohol group, C=O vibrations at 1110.8 $cm^{-1}$, and 1107.0 $cm^{-1}$, and 1703.4 $cm^{-1}$ suggest the presence of an ester group, C-O vibrations at 1218.8 $cm^{-1}$ suggests the presence of a cyclic ether, and C-H vibrations at 954.2 $cm^{-1}$ and 890.8 $cm^{-1}$ suggests the presence of alkenes. These peaks are notable because they highlight the presence and significance of span 60 in the formulation. Similar vibrations at 954.2 $cm^{-1}$ and 890.8 $cm^{-1}$ also suggest the presence of numerous alkene groups in the structure of CP. The N-H vibrations at 1617.7 $cm^{-1}$ imply the presence of an amine group, which is present only in the structure of CP. The shift in C=O vibrations to 1751.9 $cm^{-1}$ suggests possible interactions between CP and other excipients. Overall, the similarity of the position and appearance of the spectra within CP-excipient pairings, as well as the retention of bands indicating CP throughout the storage period, suggests that the formulation is compatible.

**3.2. Optimization parameters**

**Appendix D** shows the calibration curve for CP and the equation developed using linear regression to compute the equivalent drug concentration based on the absorbance of each sample. An $R^2$ value of 0.9957 indicates that the curve is linear, and that the resulting equation is valid. **Appendix E** displays niosomal formulation and drug entrapment parameters, including EE, DE, and ΔG°. Formulation 5 (F5) exhibited the highest entrapment and diffusion efficiency, with values of 72.49 ± 0.23% and 804.8 ± 145.4 mcg/hr, respectively. The results confirm the earlier observation by Uchegbu et al. that the molar quantity of the surfactant is strongly correlated with niosomal entrapment and diffusion, accompanied by a consistent reduction in energy consumption[15]. The increased drug entrapment is attributed to the enhanced bilayer fluidity of the niosomes formed above the phase transition temperature of Span 60 (50 °C). At this temperature, the

surfactant molecules become more mobile, promoting proper vesicle formation and enabling more efficient drug entrapment within the bilayer. In addition, the balance of mutual repulsion between surfactant layers plays a crucial role in niosomal entrapment and stabilization. As elaborated by Kazi et al., when the drug interacts with the surfactant head groups, electric charges may develop, leading to mutual repulsion that increases vesicle size and potentially enhances entrapment efficiency[16]. This principle supports the incorporation of cholesterol and DCP into the formulation. Cholesterol, through its hydroxyl groups, can form hydrogen bonds with the hydrophilic regions of the surfactant, thereby increasing bilayer rigidity and cohesion[17]. Meanwhile, DCP, a negatively charged molecule, induces electrostatic repulsion between vesicles, which prevents aggregation or fusion and enhances the overall stability of the niosomal system[8]. Furthermore, increasing the amount of Span 60 improves vesicle formation, which contributes to greater thermodynamic stability of the system. This is supported by the observed decrease in Gibbs free energy (ΔG), indicating that the process becomes more spontaneous and shifts toward a more stable energy state[16]. As a result, F5 exhibited the lowest free energy change during niosome formation. In isolated systems such as niosomes and liposomes, no energy is usually exchanged with the environment, resulting in non-spontaneous processes during drug entrapment due to decreased entropy. This observation contradicts the third law of thermodynamics, which states that the entropy of a pure crystalline drug is zero due to spontaneous processes involving interconversion from amorphous to crystalline states. Furthermore, $f_2$ values below 50 and $f_1$ values above 15 confirmed the significant difference in diffusion efficiency between F5 and the other formulations[18].

### 3.3. *In vitro* drug release

**Figure 1** presents the *in vitro* release kinetics of the loaded niosomal formulations over eight hours, which are consistent with the findings reported by Zaki et al. and Akbarzadeh et al.[14,19]. In agreement with previous research, F5 which contained the highest amount of Span 60 and exhibited the highest EE, also released the least amount of CP. Although Formulation 1 showed the lowest CP release at certain time points, its release profile displayed non-cumulative fluctuations, including decreases in drug release, which are not expected in a cumulative release profile and may be attributed to experimental inconsistencies or measurement errors. In contrast, Formulation 5 demonstrated a consistent, gradual increase in drug release, characteristic of a controlled and sustained release system. Therefore, F5 was selected as the formulation that released the least cumulative amount of CP over time. These findings reinforce the notion that surfactant type and concentration play a crucial role in drug entrapment and release behavior.

Numerous studies have reported that among commonly used surfactants, Span 60 demonstrates the highest EE[19-21]. This is largely attributed to its high phase transition temperature, which facilitates the formation of

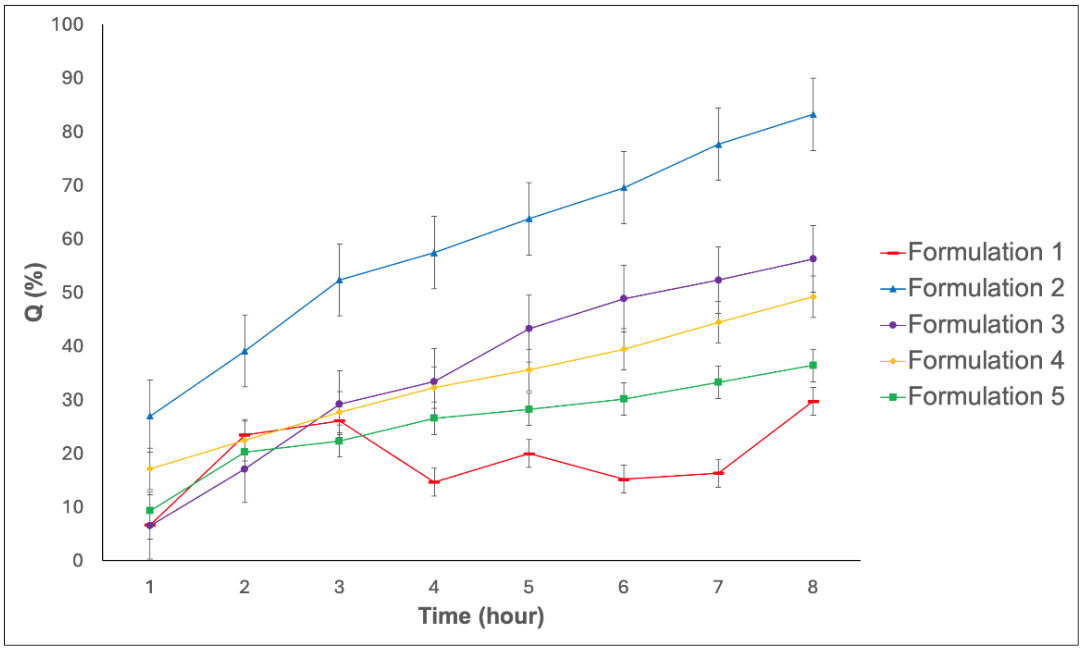


**Figure 1.** Cumulative release profile of CP from five niosomal formulations over 8 hours using USP Dissolution Apparatus 1, with samples collected hourly in PBS (pH 7.4, 37 ± 0.5°C) and CP quantified via UV-Vis spectrophotometry.

a rigid bilayer structure capable of retaining greater amounts of drug while minimizing diffusion across the membrane, thereby resulting in sustained drug release[19]. Additionally, the alkyl chain length of the surfactant plays a critical role in modulating drug release; surfactants with longer alkyl chains tend to form less permeable bilayers at physiological temperatures, leading to prolonged release profiles[20]. This observation is supported by the findings of Alyami et al., who reported that among pilocarpine-loaded niosomal formulations prepared with various types of Spans, Span 60 produced the largest vesicle size and the highest EE[22]. These findings collectively justify the selection of Span 60 as the surfactant of choice in the present formulation. Other factors that contribute to prolonged drug release in niosomes include vesicle size[23], cholesterol content, and the method of preparation. Higher cholesterol levels enhance bilayer rigidity and reduce membrane permeability, thereby limiting osmotic alterations and promoting greater drug retention within the niosomes. Additionally, the preparation method significantly influences EE and subsequent drug release behavior. Ugorji et al. reported that niosomes prepared using the thin-film hydration method exhibited significantly higher EE compared to those produced by other methods[21].

After fitting the results to multiple models to describe the primary mechanism for drug release, the $R^2$ values were calculated and presented in **Appendix F**. The findings show that the primary mechanism involved in drug release in niosomal formulations best fits the Korsmeyer-Peppas model. The model involves four mechanisms developed to comprehend the complex mechanisms of polymeric nanoparticles, such as niosomes and liposomes in controlled and sustained drug release, as measured by the calculated diffusion or release exponent (n). Data shows that the values for all niosomal formulations ranged from 0.50 to 1.00, indicating an anomalous, non-Fickian diffusion mechanism. This implies that the mechanism for drug release is a combination of diffusion and polymer swelling, resulting in non-linear drug release over time. Such behavior had been observed in a study employing the development of niosomes containing tyloxapol[12].

Based on the EE and *in vitro* release profiles of the loaded niosomal formulations, F5 was selected as the ONF for further characterization.

### 3.4. Solid state analysis

The ONF exhibited a PS of 223.16 ± 10.05 nm and a PDI of 0.23 ± 0.02, indicating a relatively uniform particle distribution. The method of preparation, as well as the type and amount of components utilized, can all influence the PS and PDI of niosomes. A study on niosomes containing fluorouracil prepared using various methods found that the thin film hydration method resulted in formulations with the lowest PS and PDI[21]. In addition to having higher EE and superior drug release profiles, niosomes formed using span 60 have a smaller particle size, similar to a study on niosomes containing gallic acid[24]. Notably, the inclusion of CP reduced niosomal size due to a stronger lipid bilayer developing between the drug and the excipients. The particle size significantly impacts drug absorption and subsequent distribution throughout the body. A low PDI, as evidenced by the samples, suggests particle size uniformity and higher entrapment efficiency, supporting the previously supplied findings.

A zeta potential test was performed to determine the stability of the formulation and behavior in the presence of various substances in the body. The ONF exhibited a ZP of −47.69 ± 5.28 mV, indicating favorable electrostatic stability. The negative charge of the findings represents their stability and reduced risk of aggregation, which is caused by the adsorption of certain ions on the vesicle surface. A work by Zolghadri et al. supports the relative stability of ONF based on its zeta potential, stating that levels greater than +35 or -35 mV are stable[24].

The SEM photomicrograph in **Figures 2A** and **2B** illustrates that the niosomes exhibit a large, spherical, and vesicular morphology. Drug entrapment ensured the stabilization of the nanoparticle network, which resembled the bilipid layer of cell membranes, with increased rigidity conferred by a higher molar quantity of span 60. This observation is consistent with the production of SMVs with larger pore diameters, whose permeability varies with storage and time.

The C-H vibrations at 2920.0 $cm^{-1}$, 2860.6 $cm^{-1}$, and 1379.9 $cm^{-1}$, C=O vibrations at 1645.4 $cm^{-1}$, and C-C vibrations at 722.2 $cm^{-1}$ indicate the presence of methyl and carbonyl groups, which are present in the excipients comprising the niosome. The C-O vibrations at 1055 $cm^{-1}$ indicate the presence of cyclohexane, a key part of the structure of cholesterol. N-H vibrations at 3419.8 $cm^{-1}$ and C-N vibrations at 1177.6 $cm^{-1}$ indicate the presence of amine, SCN vibrations at 2075.5 $cm^{-1}$ indicate the presence of an isothiocyanate group, and C=O vibrations at 1738.3 $cm^{-1}$ indicate the presence of carbonyl groups, which are notable because these groups are only found in the structure of CP[25]. The similarity between the spectra of blank niosomes and ONF in **Figure 3** indicates that the drug may be trapped inside the ligand, consistent with the findings of Aguilar-Jiménez and her group[26]. The differences in signals between the three samples indicate that the ONF is distinct from the original molecules.

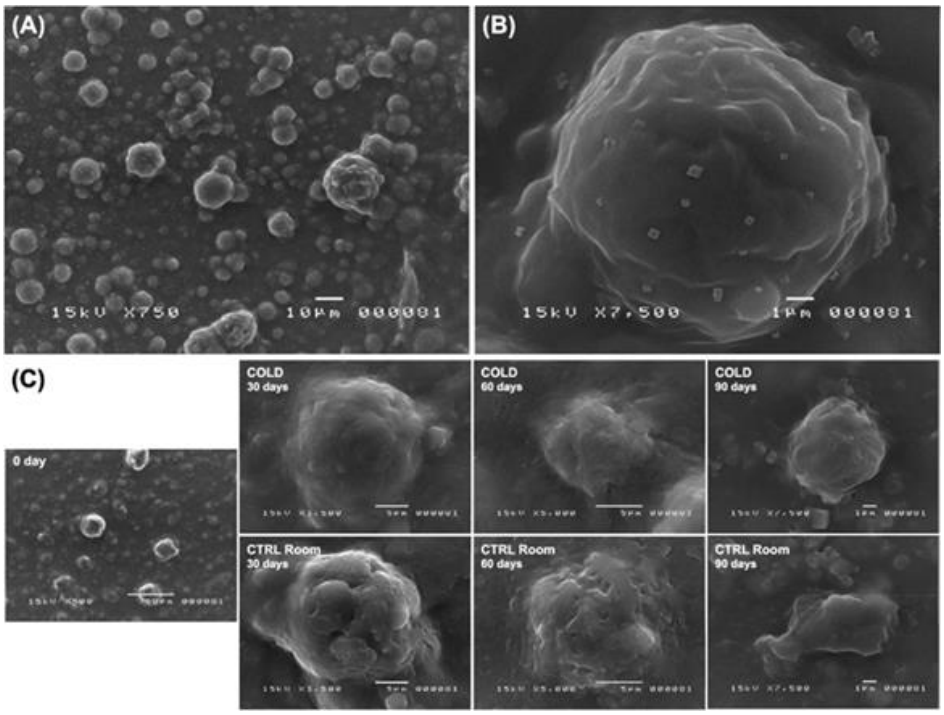


**Figure 2.** SEM images of the optimized niosomal formulation (ONF): Freshly prepared ONF imaged at varying magnifications after gold coating under vacuum **(A–B)**; Morphological changes in ONF stored under cold and controlled room conditions over 90 days **(C)**.

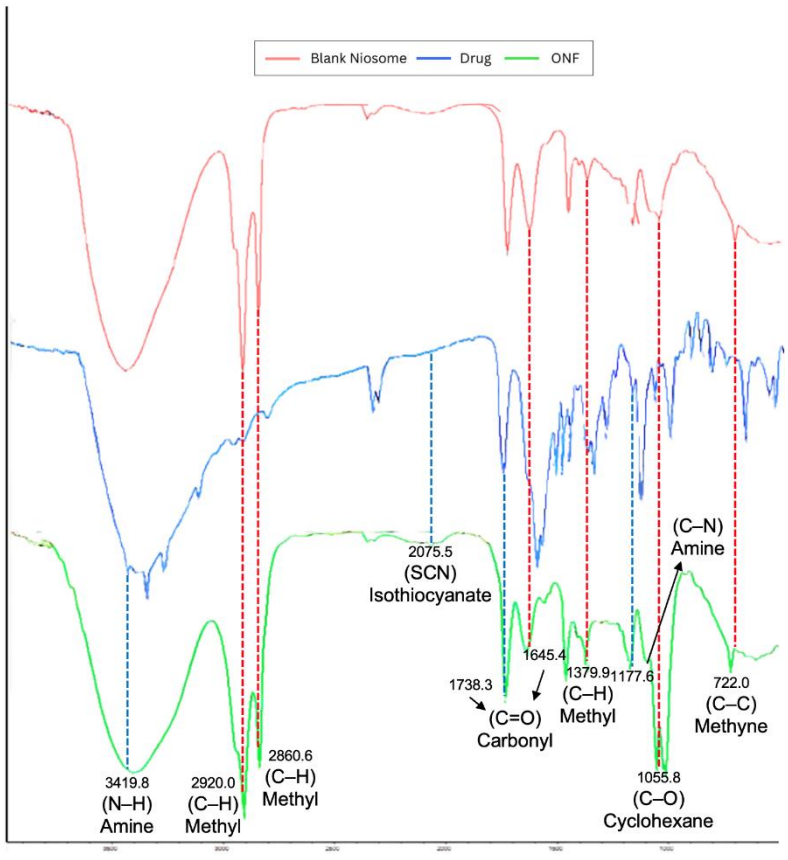


**Figure 3.** FTIR spectra of the CP **(A)**, CP-loaded ONF **(B)**, and blank niosomes **(C)**, confirming successful drug entrapment.

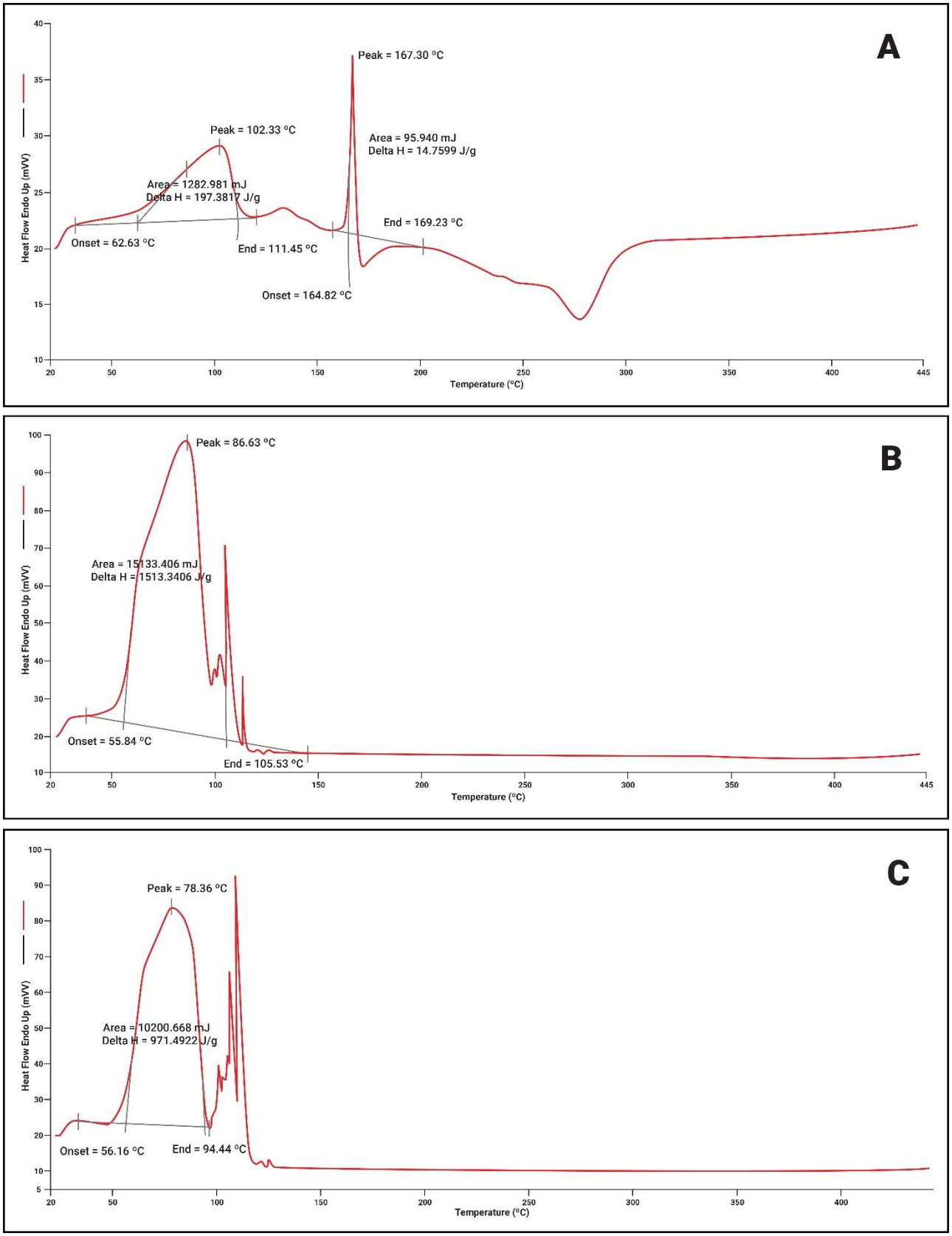


**Figure 4.** DSC thermograms of CP **(A)**, ONF **(B)**, and blank niosomes **(C)**, reveal changes in thermal behavior, indicating successful drug encapsulation within the niosomal matrix.

### 3.5. Differential scanning calorimetry (DSC) analysis

**Figure 4** presents the DSC thermograms of CP, ONF, and blank niosomes. The thermogram of pure CP (**Figure 4A**) displays two pronounced endothermic peaks. The first peak, observed at 102.33°C with an enthalpy change (ΔH) of 197.381 J/g, corresponds to the melting point of the crystalline drug. This is further

supported by a second sharp endothermic event at 167.30°C (ΔH = 14.7599 J/g), indicative of its high crystallinity[27].

In contrast, the thermogram of the optimized niosomal formulation (**Figure 4B**) shows a broad endothermic peak at 86.63°C, with a significantly higher enthalpy change (ΔH = 1513.3406 J/g). Notably, the absence of CP's characteristic melting peaks suggests a loss of crystallinity and a possible transformation to an amorphous or molecularly dispersed form within the niosomal bilayer. This thermal shift, along with the disappearance of sharp peaks, implies strong drug–excipient interactions and supports successful drug encapsulation[28].

The DSC curve of the blank niosomes (**Figure 4C**) exhibits a major endothermic peak at 78.36°C (ΔH = 971.4922 J/g), corresponding to the phase transition of surfactant and cholesterol components. The similarity between the thermal profiles of ONF and blank niosomes indicates that the matrix governs the overall thermal behavior of the formulation. This further confirms the entrapment of CP within the vesicular structure, rather than existing in its crystalline form[29].

Collectively, these thermal transitions and the disappearance of CP's melting endotherms in the ONF thermogram provide strong evidence of successful encapsulation and suggest potential molecular dispersion of CP within the niosomal bilayer.

### 3.6. Stability testing

**Figure 2C** displays SEM photomicrographs of ONF stored at controlled temperature, revealing niosomal breakdown around the second month, as supported by a significant loss of 23.96% of its initial EE. The neutralization of the surface charge of surfactant molecules upon breakdown, as well as the increased molecular motion and collision frequency at high temperatures, resulted in the gradual disintegration of niosomes, reducing their ability to entrap the drug and inducing leakage[30]. **Figure 5** shows a yellowish-white color caused by the conversion of leaked CP to pyridine and Δ-2 isomers through temperature-dependent electrophilic and nucleophilic assaults hydrolyzing the beta-lactam ring[31]. The FTIR spectra in **Appendix G** supports this explanation by revealing bands indicating CP, such as C=O vibrations at 1111.0 $cm^{-1}$, 1106.9 $cm^{-1}$, and 1702.9 $cm^{-1}$, C-H vibrations at 954.0 $cm^{-1}$, and N-H vibrations at 1613.9 $cm^{-1}$, indicating the presence of a heterocyclic nitrogen ring such as pyridine[25]. The presence of these two compounds is also evidenced by a steady increase in pH to 6.13. The ONF also declined in ZP, reaching -33.69 ± 1.36 mV. ZP is determined by the electrostatic repulsion of adjacent particles, which increases ion flow and decreases viscosity as the temperature rises.

After three months of storage at cold temperatures, ONF retained its original, milky-white color and lost 0.61% of its initial EE, with SEM photomicrographs indicating niosomal integrity. The pH increased slightly to 6.03, and FTIR spectra revealed bands found only in the excipients comprising the niosomes. These results in **Figure 6** demonstrate the retention of CP and the preservation of niosomal integrity, resulting in minimal drug release.

Overall, the findings imply that temperature plays an important role in niosomal stability.

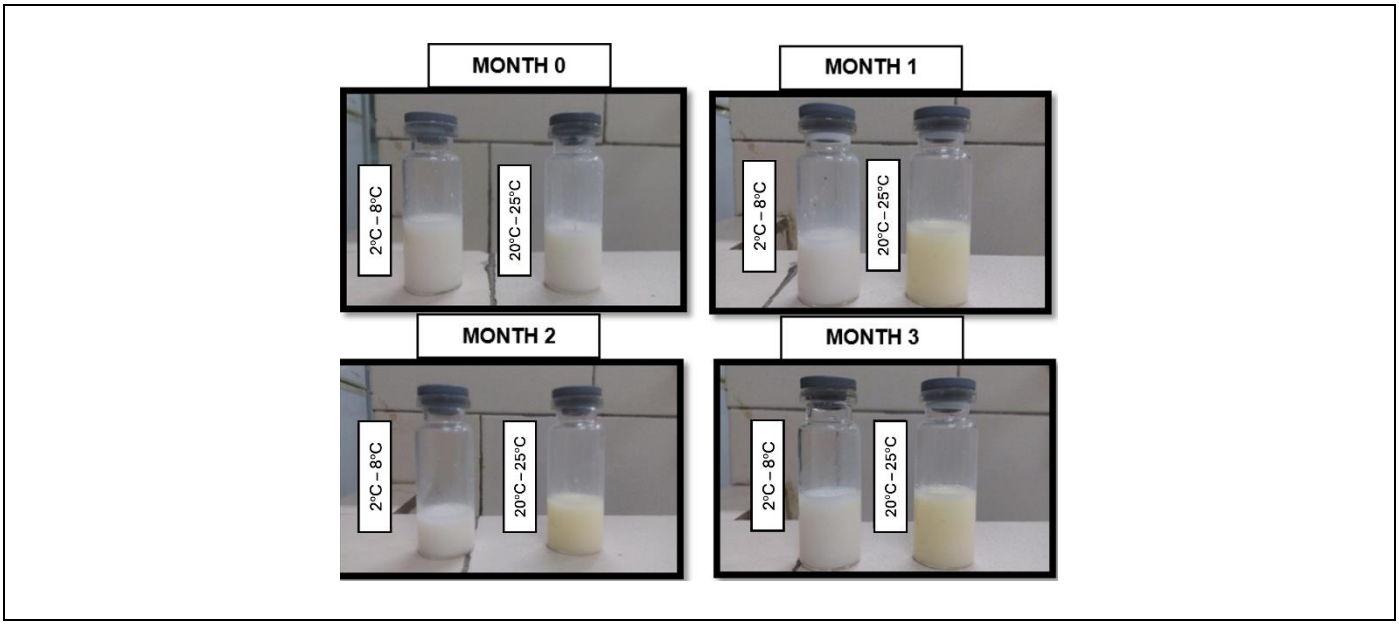


**Figure 5.** Organoleptic evaluation of ONF stored at cold and controlled room temperature over 3 months showing visual changes in color and appearance.

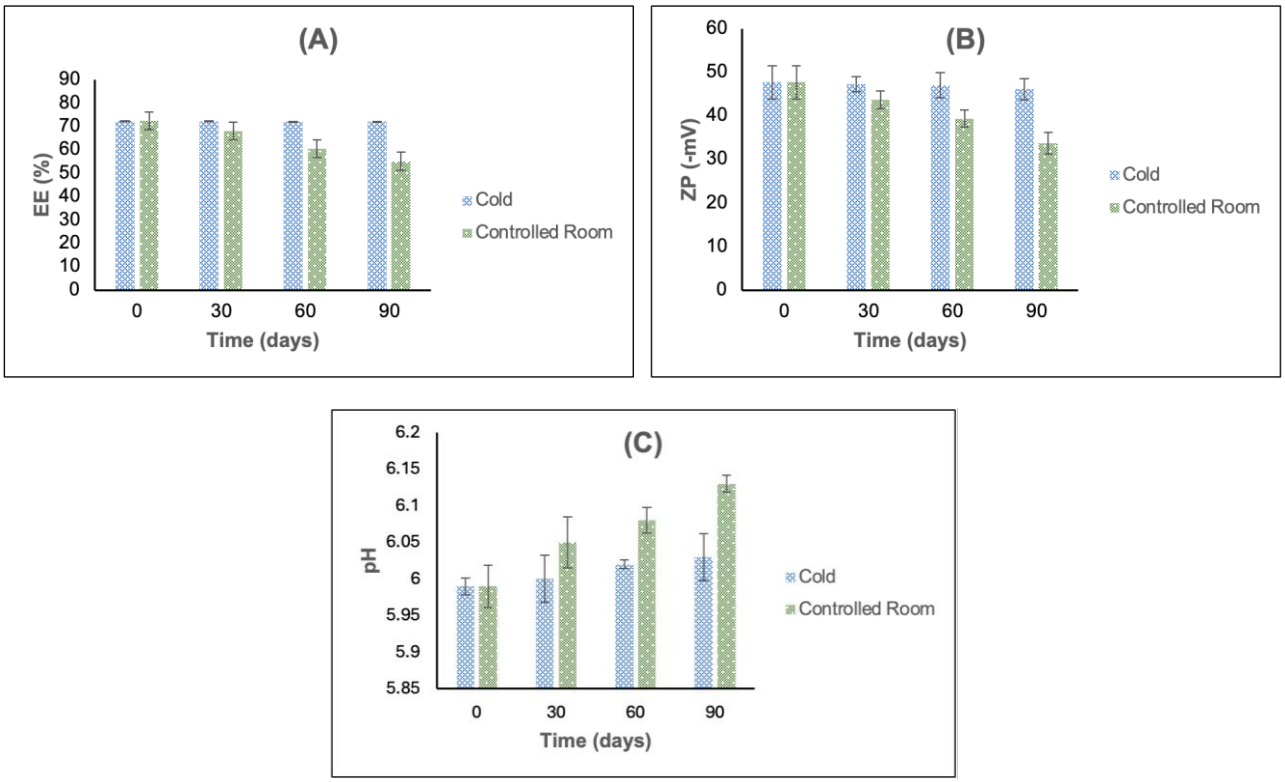


**Figure 6.** Stability evaluation of ONF stored under cold and controlled room conditions over 90 days, showing changes in entrapment efficiency **(A)**, zeta potential **(B)**, and pH **(C)**.

### 3.7. Antibacterial assay

**Figure 7** compares the results of the agar well diffusion assay for the ONF, free CP, and blank niosomes against selected nosocomial pathogens. The ONF exhibited ZOIs ranging from 26 mm to 40 mm, which were notably larger than those of the free drug (20 mm to 37 mm). These results confirm that niosomal encapsulation enhanced the antibacterial activity of CP against the tested pathogens. The improved antibacterial activity of the ONF can be attributed to a combination of improved physicochemical properties and controlled drug delivery behavior. The high EE ensured a greater proportion of the active compound was retained and

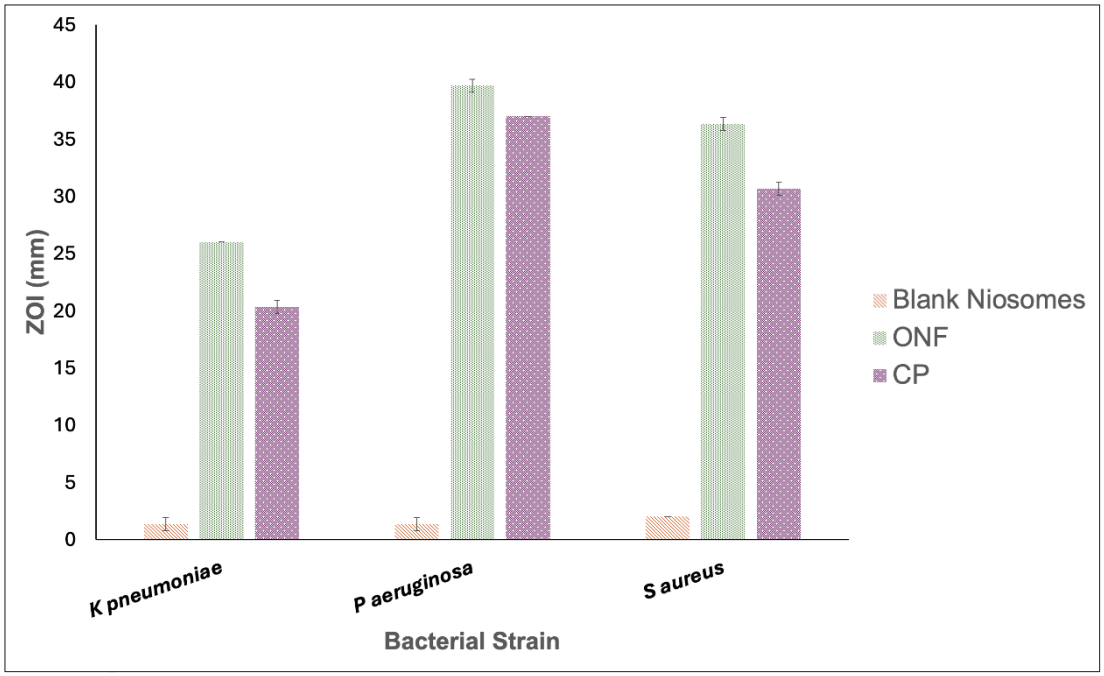


**Figure 7.** ZOI of blank niosomes, CP, and ONF against *K. pneumoniae*, *P. aeruginosa*, and *S. aureus* determined using the well diffusion assay.

made bioavailable, while the uniform particle size and highly negative zeta potential contributed to formulation stability and facilitated effective diffusion into the surrounding medium. The sustained release profile, governed by a non-Fickian diffusion mechanism, allowed for prolonged antimicrobial action and consistent exposure of bacterial cells to the drug over time. Furthermore, the nanoscale dimensions and amphiphilic nature of the vesicles likely promoted stronger interactions with bacterial membranes, enhancing cellular uptake and increasing local drug concentration at the infection site. These properties collectively result in improved diffusion, membrane fusion, and drug retention, explaining the enhanced antibacterial activity observed. However, certain *Escherichia coli* strains express the New Delhi metallo-β-lactamase-1 (NDM-1) enzyme, which confers resistance to carbapenems and cephalosporins[32]. As a result, none of the tested samples exhibited significant activity against this resistant bacterium.

## 4. CONCLUSION

Our study is the first to report the subsequent improvement in the antibacterial activity of CP through niosomal entrapment. The ONF with the highest amount of span 60 exhibited the highest EE and DE, highlighting its importance in producing the most rigid niosomes that will release the drug in the slowest, most controlled manner. The FTIR studies suggest drug-excipient compatibility and the relative stability of the formulation at common storage conditions. The ONF also demonstrated greater antibacterial activity against selected nosocomial pathogens than the free drug due to the non-Fickian release mechanisms and enhanced intrabacterial drug release caused by its niosomal structure. However, testing for minimum inhibitory and bactericidal concentrations is recommended to provide greater insight into the formulation's action. Lastly, accelerated stability studies and toxicity tests are recommended to determine the suitability of the formulation for commercial use. This study establishes a framework for future advances in antimicrobial drug delivery, which are crucial in combating the progressive rise of drug-resistant microbes.

## 5. ACKNOWLEDGEMENTS

The authors would like to thank Ms. Helen Jenina C. Sto. Domingo for her assistance with interpreting and visualizing the FTIR results.

**Author contributions**

JKTE managed and directed the study throughout. JKTE, SAA, JKETE, and JDMM conducted the study and contributed equally to the manuscript writing. GQDG and MSA directed and led the researchers in conducting the study.

**Funding**

None to declare.

**Conflict of interest**

The authors declare that they have no conflicts of interest.

**Ethical approval**

None to declare.

**Article info:**

Received February 12, 2025
Received in revised form July 20, 2025
Accepted August 21, 2025

## REFERENCES

1. Reardon S. WHO warns against “post-antibiotic” era. Nature. 2014;15:135-8.
2. Ahmed SK, Hussein S, Qurbani K, Ibrahim RH, Fareeq A, Mahmood KA, et al. Antimicrobial resistance: Impacts, challenges, and future prospects. J Med Surg Public Health. 2024;2:100081.
3. El Mammery A, Ramírez de Arellano E, Cañada-García JE, Cercenado E, Villar-Gómara L, Casquero-García V, et al. An increase in erythromycin resistance in methicillin-susceptible *Staphylococcus aureus* from blood correlates with the use of macrolide/lincosamide/streptogramin antibiotics. EARS-Net Spain (2004-2020). Front Microbiol. 2023;14:1220286.
4. Barani M, Paknia F, Roostaee M, Kavyani B, Kalantar-Neyestanaki D, Ajalli N, et al. Niosome as an effective nanoscale solution for the treatment of microbial infections. Biomed Res Int. 2023;2023:9933283.
5. Hemmati J, Chegini Z, Arabestani MR. Niosomal-based drug delivery platforms: a promising therapeutic approach to fight *Staphylococcus aureus* drug resistance. J Nanomater. 2023;2023:5298565.
6. Paseban K, Noroozi S, Gharehcheloo R, Haddadian A, Falahi Robattorki F, Dibah H, et al. Preparation and optimization of niosome encapsulated meropenem for significant antibacterial and anti-biofilm activity against methicillin-resistant *Staphylococcus aureus* isolates. Heliyon. 2024;10(16):e35651.
7. Shiri S, Gharanjig K, Tahghighi A, Hosseinnezhad M, Etezad M. Formulation and characterization of BBR loaded niosomes using saponin as a nonionic biosurfactant investigating synergistic effects to enhance antibacterial activity. Sci Rep. 2025;15(1):5231.
8. Moammeri A, Chegeni MM, Sahrayi H, Ghafelehbashi R, Memarzadeh F, Mansouri A, et al. Current advances in niosomes applications for drug delivery and cancer treatment. Mater Today Bio. 2023;23:100837.
9. Bagheri A, Chu BS, Yaakob H. Niosomal drug delivery systems: Formulation, preparation and applications. World Appl Sci J. 2014;32:1671-85.
10. Nasseri B. Effect of cholesterol and temperature on the elastic properties of niosomal membranes. Int J Pharm. 2005;300(1-2):95-101.
11. Hu C, Rhodes DG. Proniosomes: a novel drug carrier preparation. Int J Pharm. 1999;185(1):23-35.
12. Mehta SK, Jindal N. Tyloxapol niosomes as prospective drug delivery module for antiretroviral drug nevirapine. AAPS PharmSciTech. 2015;16(1):67-75.

13. Sapte S, Pore Y. Inclusion complexes of cefuroxime axetil with β-cyclodextrin: Physicochemical characterization, molecular modeling and effect of l-arginine on complexation. J Pharm Anal. 2016;6(5):300-6.
14. Zaki RM, Ali-Adel A, Menshawe SF, ElBary AA. Formulation and evaluation of diacerine loaded niosomes. Int J Pharm Pharm Sci. 2014;6(2):515-21.
15. Uchegbu IF, Vyas SP. Non-ionic surfactant based vesicles (niosomes) in drug delivery. Int J Pharm. 1998;172:33-70.
16. Kazi KM, Mandal AS, Biswas N, Guha A, Chatterjee S, Behera M, et al. Niosome: A future of targeted drug delivery systems. J Adv Pharm Technol Res. 2010;1(4):374-80.
17. Gharbavi M, Amani J, Kheiri-Manjili H, Danafar H, Sharafi A. Niosome: A Promising Nanocarrier for Natural Drug Delivery through Blood-Brain Barrier. Adv Pharmacol Sci. 2018;2018:6847971.
18. Patterlini V, Guareschi F, D'Angelo D, Baldini S, Meto S, Mostafa Kamal D, et al. Clinically relevant characterization and comparison of Ryaltris and other anti-allergic nasal sprays. Pharmaceutics. 2024;16(8):989.
19. Akbarzadeh I, Keramati M, Azadi A, Afzali E, Shahbazi R, Chiani M, et al. Optimization, physicochemical characterization, and antimicrobial activity of a novel simvastatin nano-niosomal gel against *E. coli* and *S. aureus*. Chem Phys Lipids. 2021;234:105019.
20. Mansouri M, Khayam N, Jamshidifar E, Pourseif T, Kianian S, Mirzaie A, et al. Streptomycin Sulfate-Loaded Niosomes Enables Increased Antimicrobial and Anti-Biofilm Activities. Front Bioeng Biotechnol. 2021;9:745099.
21. Ugorji OL, Umeh ONC, Agubata CO, Adah D, Obitte NC, Chukwu A. The effect of noisome preparation methods in encapsulating 5-fluorouracil and real time cell assay against HCT-116 colon cancer cell line. Heliyon. 2022;8(12):e12369.
22. Alyami H, Abdelaziz K, Dahmash EZ, Iyire A. Nonionic surfactant vesicles (niosomes) for ocular drug delivery: development, evaluation and toxicological profiling. J Drug Deliv Sci Technol. 2020;60:102069.
23. Pando D, Beltran M, Gerone I, Matos M, Pazos C. Resveratrol entrapped niosomes as yoghurt additive. Food Chem. 2015;170:281-87.
24. Zolghadri S, Asad AG, Farzi F, Ghajarzadeh F, Habibi Z, Rahban M, et al. Span 60/cholesterol niosomal formulation as a suitable vehicle for gallic acid delivery with potent *in vitro* antibacterial, antimelanoma, and anti-tyrosinase activity. Pharmaceuticals (Basel). 2023;16(12):1680.
25. Nandiyanto ABD, Oktiani R, Ragadhita R. How to Read and Intepret FTIR Spectroscope of Organic Material. Sci Technol Indones. 2019;4(1):97-118.
26. Aguilar-Jiménez Z, González-Ballesteros M, Dávila-Manzanilla SG, Espinoza-Guillén A, Ruiz-Azuara L. Development and *in vitro* and *in vivo* evaluation of an antineoplastic copper(ii) compound (Casiopeina iii-ia) loaded in nonionic vesicles using quality by design. Int J Mol Sci. 2022;23(21):12756.
27. Perlovich GL, Volkova TV, Bauer-Brandl A. Towards an understanding of the molecular mechanism of solvation of drug molecules: a thermodynamic approach by crystal lattice energy, sublimation, and solubility exemplified by paracetamol, acetanilide, and phenacetin. J Pharm Sci. 2006;95(10):2158-69.
28. Ghanbari E, Picken SJ, van Esch JH. Analysis of differential scanning calorimetry (DSC): determining the transition temperatures, and enthalpy and heat capacity changes in multicomponent systems by analytical model fitting. J Therm Anal Calorim. 2023;148:12393-409.
29. Uchegbu IF, Florence AT. Non-ionic surfactant vesicles (niosomes): Physical and pharmaceutical chemistry. Adv Colloid Interface Sci. 1995;58(1):1-55.
30. Sangkana S, Eawsakul K, Ongtanasup T, Boonhok R, Mitsuwan W, Chimplee S, et al. Preparation and evaluation of a niosomal delivery system containing *G. mangostana* extract and study of its anti-*Acanthamoeba* activity. Nanoscale Adv. 2024;6(5):1467-79.
31. Servais H, Tulkens PM. Stability and compatibility of ceftazidime administered by continuous infusion to intensive care patients. Antimicrob Agents Chemother. 2001;45(9):2643-7.
32. Lv H, Zhu Z, Qian C, Li T, Han Z, Zhang W, et al. Discovery of isatin-β-methyldithiocarbazate derivatives as New Delhi metallo- β-lactamase-1 (NDM-1) inhibitors against NDM-1 producing clinical isolates. Biomed Pharmacother. 2023;166:115439.